Tracing the History of LINE and SINE Extinction in Sigmodontine Rodents

Lei Yang[1, 2, 3] and Holly A. Wichman[1, 2]

[1, 2]Department of Biological Sciences & Institute for Bioinformatics and Evolutionary Studies, University of Idaho, Moscow, Idaho, United States of America

[3]Present address: Department of Biology, Pennsylvania State University, University Park, Pennsylvania, United States of America

Corresponding author: Holly A. Wichman

Email: hwichman@uidaho.edu

Fax: +1(208)885-7905

Phone: +1(208)885-7805

Running title: History of LINE and SINE extinction

Abstract

Background: L1 retrotransposons have co-evolved with their mammalian hosts for the entire history of mammals and currently make up to 20% of a typical mammalian genome. B1 retrotransposons are dependent on L1 for retrotransposition and span the evolutionary history of rodents since their radiation. L1s were found to have lost their activity in a group of South American rodents, the Sigmodontinae, and B1 inactivation preceded the extinction of L1 in the same group. Consequently, a basal group of sigmodontines have active L1s but inactive B1s and a derived clade have both inactive L1s and B1s. It has been suggested that B1s became extinct during a long period of L1 quiescence and that L1s subsequently reemerged in the basal group.

Results: Here we investigate the evolutionary histories of L1 and B1 in the sigmodontine rodents and show that L1 activity continued until after the split of the L1-extinct clade and the basal group. After the split, L1s had a small burst of activity in the former group, followed by extinction. In the basal group, activity was initially low but was followed by a dramatic increase in L1 activity. We found the last wave of B1s retrotransposition was large and probably preceded the split between the two rodent clades.

Conclusions: Given that L1s had been steadily retrotransposing during the time corresponding to B1 extinction and that the burst of B1 activity preceding B1 extinction was large, we conclude that B1 extinction was not a result of L1 quiescence. Rather, the burst of B1 activity may have contributed to L1 extinction both by competition with L1 and by putting strong selective pressure on the host to control retrotransposition.

Background

LINEs (Long INterspersed Elements) are autonomous non-LTR (non-long terminal repeat) retrotransposons that move through an RNA intermediate. L1 (LINE-1) is the most successful family of LINEs in eutherian mammals [1] and make up ~20% of a typical mammalian genome [2, 3]. A functional full-length L1 is typically 6,000-7,000 bp long and composed of a 5' untranslated region (5'UTR) harboring an RNA polymerase II promoter, two non-overlapping open reading frames (ORFs) known as ORF1 and ORF2 and a 3'UTR followed by a poly-adenosine sequence [4]. The structure of L1 can be diverse among different mammals, particularly in the 5' UTR and ORF1 [5]. The ORF-encoded proteins are strictly required for L1 retrotransposition and are highly *cis*-preferential [6, 7]. L1s are adenosine rich (~40%) on their coding strand, which results in biased codon usage compared to host genes [8, 9], elongation defects [10], and premature RNA splicing [11]. This A-richness contributes to the inefficiency of L1 retrotransposition and is proposed to regulate the genes in their vicinity [10].

SINEs (Short INterspersed Elements) are relatively short non-autonomous, non-LTR transposable elements. SINEs do not encode proteins for their own retrotransposition and depend on the reverse transcriptase encoded by other transposable elements such as LINEs [12, 13]. Although L1s are highly *cis*-preferential [6, 7], SINEs can take advantage of L1-encoded proteins for their own retrotransposition [12-14]. Despite their short length, SINEs account for ~10% of a typical mammalian genome due to their high copy numbers [2, 3]. Among the ~70 SINE families found in mammals [15], B1 is the most abundant in mouse [3] and possibly most rodent species [16], occupying ~3% of the mouse genome [3]. B1s derived from the RNA component of signal recognition particle 7SL RNA [17, 18] and share features with its ancestors – a functional B1 is ~150 bp long and transcribed by RNA polymerase III with the aid of its two

transcription factor binding boxes [19, 20]. B1 sequences are rich in CpG sites, which are methylated and thus prone to mutation in mammalian genomes [21], and the elevated mutation rate is pronounced compared to the A-rich L1s. Because the majority of new L1 and B1 inserts are neutrally-evolving pseudogenes, the CpG-rich B1 sequences decay faster than the A-rich L1 sequences.

Both L1 and B1 have long histories of co-evolution with their host genomes. Unlike some transposable elements, there is no known targeted mechanism for L1s excision and thus L1s persist in the genome unless they are removed by non-specific mechanisms. The oldest L1s trace back to the common ancestor of placental mammals and marsupials, ~160 MYA [1, 22]. L1s evolve as master lineages so that a single or a few lineages are responsible for the total retrotransposition in a short time window [23-26]. New master elements replace the old ones, eventually dominating retrotransposition, and this replacement process happens recurrently. B1s are younger than L1s, having arisen just before the divergence of the common ancestor of rodents, ~65 MYA [27], and they are specific to rodents. Other SINEs, including B2, B4 and ID elements, are also present in rodent genomes [16]. SINE families have been interacting with L1s for more than 100 MYA, and fossil remnants of extinct SINE families are detectable in well-characterized mammalian genomes [15, 28]. Despite being under strict regulation, L1 and B1 make up approximately a quarter of a typical rodent genome [3]. For example, in the mouse genome, there are ~599,000 total copies of L1, responsible for ~19% of the genome [3], of which ~3,000 copies are potentially functional [29], and ~564,000 copies of B1s, responsible for ~3% of the genome [3].

LINEs and SINEs have considerable impact on the mammalian genome, although they were traditionally viewed as “junk DNA”. As LINEs and SINEs, including L1s and B1s,

retrotranspose and recombine, they introduce genome instability [30], cause disease [31] and may occasionally be co-opted by the host to serve certain functions, such as their proposed roles in neuro-plasticity [32, 33], X chromosome inactivation [34, 35], regulatory functions [36, 37], DNA break-repair [38] and genome organization [39, 40]. Due to the deleterious effects of LINEs and SINEs on the genome, the hosts have evolved many mechanisms to defend against them [41-45]. In addition, the fact that L1 doesn't encode all the enzymatic components required for retrotransposition could result in ongoing competition between L1s and the host for these required host factors [46, 47]. Host defense against L1s and B1s are especially strong in germline cells due to germline-specific host defense mechanisms, so that only a limited number of new copies are inserted in each generation [48, 49]. L1s and B1s are both epigenetically silenced [50, 51] and under the control of small RNAs [52], which are specifically expressed in germline cells.

Since L1 retrotransposition is under strict control by multiple host defenses, it might seem reasonable for the host to occasionally win the evolutionary arms race with L1s, resulting in loss of L1 activity (L1 extinction). L1s are not known to move horizontally, so such extinctions would affect all derived host species. Two factors are of note here. First, clades with early L1 extinctions could have given rise to large mammalian lineages without L1 activity and be easily detected because of both the number of species affected and the deterioration of the remnant sequences in the genome. Secondly, recent extinctions will be difficult to differentiate from periods of L1 quiescence. To clarify the terms related to loss of L1 activity in this work, we refer to a period of low L1 activity as "quiescence" and complete loss of L1 activity as "extinction". Given the large phylogenetic impact of early extinctions, one might expect L1s to eventually become extinct in most mammalian genomes, and yet L1s have persisted throughout

105 the entire evolutionary history of their placental mammal and marsupial hosts. Thus, either most
106 L1 extinctions are either recent or rare, or mammalian lineages subject to ancient L1 extinctions
107 do not persist or they give rise to few new species. Understanding the dynamics of L1 extinction
108 will be as important as understanding the dynamics of L1 activity in sorting out the impact of
109 L1s on mammalian genome evolution.

110 Several cases of L1 extinction have been proposed in the literature [53-61] and two of
111 these are deep extinction events that cover major groups of mammals [53-57]. One of the major
112 L1 extinctions [55-57] occurred in a large group of South American rodents and includes most
113 species in Sigmodontinae. Sigmodontinae is a subfamily of the Cricetidae family, including
114 approximately 377 species classified into 74 genera in nine tribes (Figure 1) [62] and thus
115 contains to 7-8% of the estimated 5,000 mammalian species [63]. Given that B1
116 retrotransposition is dependent on that of L1, it is expected that B1s should lose their activity
117 simultaneously with L1s. However, the B1 extinction in Sigmodontinae appears to have
118 preceded that of L1s based on samples from 14 genera in five tribes [55-57], where the basal
119 genus *Sigmodon* carries inactive B1 and active L1, and the descendant genera carry both inactive
120 L1 and B1 (Figure 1). It has also been shown that loss of L1 and B1 activity follows the
121 expansion of a group of endogenous retrovirus [64, 65].

122 It was previously hypothesized by Cordaux and Batzer that the L1 can experience long-
123 term quiescence as a "stealth driver" [66], and B1 extinction could have happened during this
124 period of L1 quiescence [57]. Since B1s are more prone to mutations than the average sequence
125 due to enriched CpG content, Rinehart *et al*. [57] hypothesized that B1 was unable to
126 retrotranspose at a high enough rate during L1 quiescence to replace their active copies,
127 accumulating debilitating mutations more rapidly [21] than L1s. When a more active family of

L1 emerged in the Sigmodontini, B1 was too degenerated to retrotranspose, resulting in B1 extinction even in the presence of high L1 activity.

In this study, we investigate the evolution histories of L1 and B1 spanning the time of their extinctions and the radiation of the extant species in Sigmodontinae (Figure 1). Since the group carrying extinct L1s and B1s (Oryzomyalia, Figure 1) shares a common ancestor, we used the marsh rice rat *Oryzomys palustris* to represent this group, hereafter referred to as the "L1-extinct clade". We used the hispid cotton rat *Sigmodon hispidus* to represent the clade carrying active L1 but inactive B1, hereafter referred to as the "basal group". We used the deer mouse *Peromyscus maniculatus* to represent a closely related clade carrying both active L1 and B1, hereafter referred to as the "outgroup".

Using genome trace files from the species representing the L1-extinct clade and the basal group, we show that the activity of L1 and B1 families that precede the divergence of the clades is comparable in the current genomes of the two groups. L1 families had been steadily replaced before the split of the two groups and maintained activity after the split of the basal group and the L1-extinct clade. Shortly after this split L1 activity ceased in the L1-extinct clade but became highly active in the basal group. B1s, on the other hand, had a very large increase in activity prior to the split between the L1-extinct clade and the basal group, and there is no strong evidence of activity in the two groups following their divergence. The large burst of B1 activity just prior to extinction suggests that L1 quiescence is unlikely responsible for B1 extinction. The last wave of B1 retrotransposition is the largest detectable in the B1 evolutionary history of the group, suggesting B1s' strong competition with L1s or enhanced host defense triggered by radical B1 expansion might have contributed to the extinction of L1.

Results

To investigate the history of L1 retrotransposition in *O. palustris* and *S. hispidus*, we used COSEG [67] to identify closely related L1 groups based on shared, co-segregating sites as described in Methods. We follow the convention of COSEG to designate these groups as *subfamilies*. RepeatMasker [67] was used to initially assign genomic L1 copies to subfamilies, and seven subfamilies with no assigned sequences were removed from further consideration, leaving 47 subfamilies for further analysis.

To examine the activity of L1s in *O. palustris* and *S. hispidus*, we searched the trace files of both genomes separately with the consensus sequences of the abovementioned 47 subfamilies and identified 19,254 sequences in *O. palustris* and 90,526 in *S. hispidus*. The age of each sequence was approximated by its percent divergence from the corresponding subfamily consensus – the higher the percent divergence, the older the sequence. The peak of the distribution was used as an approximation of the age of the subfamily (Table S1). Given the possible changes of evolution rate in the detectable range of L1 evolutionary, a global conversion from percent divergence to time is challenging. However, because of the shared evolutionary history of *O. palustris* and *S. hispidus*, percent divergence is a reasonably good marker to compare the age of L1 subfamilies of the two species.

Subfamily consensus sequences were also subjected to phylogenetic analysis (Figure S1). Subsequently, phylogenetic relationships and sequence similarities between subfamilies were used to assign subfamilies to families with the stipulation that the pairwise distance between subfamilies within a family be no greater than 3.5%. This distance was determined operationally based on the divergences among phylogenetically clustered subfamilies. Clusters of subfamilies that were similar at the sequence level but differed in age were assigned to different families.

This process identified five families specific to *S. hispidus* (S1 to S5), four families shared by *O. palustris* and *S. hispidus* (OS1 to OS4) and two shared by *P. maniculatus*, *O. palustris* and *S. hispidus* (OSP1 and OSP2, Table S1). A distance-based phylogeny reflecting the relationship between L1 families is presented in Figure 2A. Individual sequences were assigned to the families to which their subfamilies belong; the age distribution within a family is based on the distance of each sequence from its subfamily consensus (Figure 3).

As expected, sequences from L1 families shared by *O. palustris* and *S. hispidus* are present in both genomes, and these shared families are fairly synchronized in time and comparable in copy number (Figure 3A). The *Sigmodon*-specific L1 families (Figure 3B, families S1-5) experienced substantial amplification after divergence from the L1-extinct clade, whereas no *Oryzomys*-specific subfamilies were identified by COSEG. The *Sigmodon*-specific subfamilies had a few sequences from the *O. palustris* genome assigned to them, but these assignments appear to be anomalous since the sequences are highly divergent from the subfamily consensus sequences (Table S1). Family OS1, the youngest shared family is of special interest. Family OS1 corresponds to a single L1 subfamily, suggesting that there was little divergence of L1s within the family. It is the last active family prior to the L1 extinction and has ~1.5-fold higher copy numbers per Gbp of sequence in *O. palustris* than in *S. hispidus*. This difference in L1 deposition between *O. palustris* and *S. hispidus* suggests that L1s remained active in the L1-extinct clade after the separation of that group from the basal group. Furthermore, L1s were more active in the lineage leading to Oryzomyalia, in which L1s eventually became extinct, than in the lineage leading to Sigmodontini. A direct comparison of the activity of the L1 families directly preceding this split (OS2), directly following the split (OS1) and at the base of the Sigmodontini (S5) is presented in Figure 4A. Thus, L1 experienced an expansion (family OS1)

in the lineage leading to Oryzomyalia immediately before L1 extinction, while the lineage leading to Sigmodontini experienced a delayed but much larger L1 expansion.

In order to study the B1 dynamics in sigmodontine rodents, we performed the analysis on B1 similar to that done on L1. Because of the short length and CpG-rich nature of B1, we required twice as many sequences to form a subfamily in the second round COSEG as described in Methods. The analysis revealed 30 subfamilies and five families of B1 in both species (Table S2). A distance-based phylogeny reflecting the relationships between B1 families is presented in Figure 2B. One of the families (OS1) is shared by *O. palustris* and *S. hispidus* and the other four (families OSP1-5) are shared by *O. palustris*, *S. hispidus* and *P. maniculatus*. All of the B1 families are shared by *O. palustris* and *S. hispidus* and the representation of these families in both genomes is fairly synchronized in time and comparable in copy number (Figure 5). Since the outgroup, represented by *P. maniculatus*, carries both active L1s and B1s, we know that B1 extinction happened after the split of the outgroup, yet the point at which B1 lost activity in the basal group is to be determined. Here we show that the peak of the most recent B1 family resides at ~11.3% in *O. palustris* and ~10.7% in *S. hispidus* (Table S2). These peaks reside in the same time window as L1 family OS2 (~11.1% in *O. palustris* and ~10.3% in *S. hispidus*, Table S1), suggesting that B1 family OS1 is coincident in time with L1 family OS2. Since L1 family OS2 is the youngest L1 family prior to the separation of the basal group and the L1-extinct clade, the last wave of B1 retrotransposition likely preceded the extinction of L1.

Discussion

In this paper we explore the tempo of L1 and B1 activity surrounding the extinction of both elements that occurred in most species within the rodent subfamily Sigmodontinae. This

work is made possible by sequencing methods that allow us to gather large amounts of sequence data and by the availability of a robust species phylogeny for the group (Figure 1). A recent phylogenetic analysis of muroid rodents [68] indicates that the tribe Sigmodontini is basal to the group and sister to the tribe Ichthyomyini. These two tribes are sister to a large, polytomic group (the Oryzomyalia) which includes the remaining five tribes; this group is the result of a rapid radiation of rodents into South America about 5 MYA [69]. Previous work indicated that L1s are extinct in the Oryzomyalia but active in the Sigmodontini, which includes one genus, *Sigmodon*, with 14 species. L1 extinction in the Oryzomyalia has been documented in 14 genera distributed across four tribes spanning this group (Figure 1) [56]. B1s are extinct in Oryzomyalia and Sigmodontini, but the status of both L1s and B1 in the intermediate tribe, Ichthyomyini, is unknown. Thus, L1 extinction from this single event likely affects between 345 and 362 species, or about 7% of all mammalian species.

We reconstructed the shared evolutionary history of L1s and B1s in Sigmodontinae in the period preceding and following extinction of these elements. Our results suggest that L1 master elements have been replaced steadily prior to the extinction of both L1 and B1. This is reflected by the consecutive series of L1 families shared by *O. palustris* and *S. hispidus* after their divergence from *Peromyscus*. B1 elements did not appear to take advantage of every wave of L1 activity, but a wave of L1 retrotransposition (family L1-OS2) corresponds to the B1 retrotransposition peak just prior to B1 extinction (B1-OS1).

There is reasonably strong evidence that L1 extinction occurred after the split between the L1-extinct clade and the basal group. A summary diagram showing the higher level of OS1 activity in *O. palustris* compared to *S. hispidus* (Figure 4A) suggests that the events leading to L1 extinction also happened after the split, rather than that a recovery occurred in *S. hispidus* as

has been previously suggested [56]. The evolutionary history of B1 in *O. palustris* and *S. hispidus* is comparable. New B1 deposition into the genome was low except for the period directly preceding B1 extinction (Figures 4B and 5). Given the short length of B1s, it is more difficult to identify subfamily clusters, so our estimation of the timing of B1 extinction is weaker than for L1. However, two lines of evidence suggest that the last burst of B1 activity occurred prior to the split between the L1-extinct and basal groups. First, the peak activity of B1OSP1 corresponds most closely to the peak activity of L1OS2, which appears to precede the split of these two rodent clades. Secondly, there is no indication of large differences of activity for any of the B1 subfamilies, as was the case for L1. We suggest that finding the status of both L1s and B1s in the Ichthyomyini lineage might be critical to resolving the timing of B1 extinction.

The most challenging part of studying transposable element evolution history in rodents is the limitation of time windows reflected by detectable sequences. The sequences detectable by RepeatMasker decrease drastically beyond 40% divergence. Since the mutation rate in the rodent lineage is one of the highest in all mammals, 40% divergence in L1 and B1 traces back to the common ancestor of sigmodontine rodents and *P. maniculatus*, while similar studies on bats [54] and primates [70, 71] trace back to the common ancestor of mammals. Fortunately, *P. maniculatus* carries both active L1s and B1s and is close enough to serve as an outgroup in this study. We were able to identify an L1 family shared by *O. palustris*, *S. hispidus* and *P. maniculatus*, family OSP1.

However, there is an advantage of studying rodents in this type of evolutionary study. Since the mutation rate in the rodent lineage is higher than that of primates and bats due to shorter generation time, evolution in L1 and B1 families reflected by a given span of divergence covers a wider window of time compared to more slowly evolving species. This gives the age

distributions of L1s and B1s higher resolution and allows us to discern subtle differences between subfamily ages.

This study is fully bioinformatics-based, but several points are important if one is to consider the underlying molecular events relevant to transpositional bursts and extinctions. L1 and B1 retrotransposition is regulated by a plethora of cellular factors [41-43, 52] and reliant on others [46, 47]. For evolutionary studies, especially the ones related to L1 and B1 extinction, the historical state of host cellular factors could dramatically change the retrotransposition landscape. Given that not all cellular factors that affect L1 and B1 retrotransposition are known and that coevolution between the elements and these cellular factors is expected, it is not currently possible to fully deduce the molecular events surrounding L1 extinction. However, from an evolutionary perspective, fixed retrotransposition events are recorded in the genome and evolve neutrally as pseudogenes unless excised or too old to be recognized. Therefore, the fossil record of L1s and B1s in the genome is a good temporal record of retrotransposition over time. However, one should keep in mind that estimation of retrotransposition rate based on historical L1 copy numbers could be affected by the excision rate of the host genome. It has been shown that the mammalian genomes have been constantly expelling sequences by various mechanisms and the excision rate varies in different clades of mammals [72]. As old insertions are not actively making new copies, they are exposed to the excision mechanisms for longer time, thus fewer copies of the older families are represented on the histogram. Old L1 and B1 copies also suffer from the recognition limitation of alignment algorithms. Detectable L1 and B1 copies are drastically reduced beyond 40% divergence.

Methods

289 *O. palustris* and *S. hispidus* genomic DNA was sequenced in two separate batches using
290 MiSeq (Illumina, Inc., San Diego, CA) at the IBEST Genomic Resources Core (University of
291 Idaho, Moscow, ID). Paired-end libraries were generated with an insert size of 450-550 bp; ~13
292 and 14 million total reads were generated for *O. palustris* and *S. hispidus*, respectively.
293 Sequences were processed with SeqyClean (https://bitbucket.org/izhbannikov/seqyclean) and the
294 paired-ends were joined with FLASH [73]. Genome coverage was equivalent to approximately
295 1.5X; 5.47 Gbp of sequence were generated for *O. palustris* and 6.06 Gbp for *S. hispidus*, but we
296 note that genome size within the sigmodontine rodents varies. Although the genome size of *O.*
297 *palustris* is not documented to our knowledge, the genome size of sister species in *Oryzomys*
298 suggests that *Sigmodon* genomes are 11-16% larger than those of *Oryzomys* [74].
299 L1 reconstruction for both species was generated based on partial genomic sequences
300 generated by 454 Pyrosequencing (Roche Applied Science, Penzberg, Germany) at the IBEST
301 Genomic Resources Core, 203 Mbp of sequence for *O. palustris* and 214 Mbp for *S. hispidus*. *P.*
302 *maniculatus* genome trace files were obtained from NCBI. Reconstruction of the 3' ends of *O.*
303 *palustris* and *S. hispidus* L1s started with a 575 bp consensus seed in the 3' half of L1 ORF2
304 generated following Cantrell *et al.* [75]. A bioinformatic pipeline for reconstructing a full length
305 L1 is described by Yang *et al*. [54]. Briefly, sequences were acquired from the genome trace
306 files based on percent identity. The overhangs of the found sequences allowed the creation of
307 new seeds at both ends of the L1 fragment and were used to initiate another round of query. In
308 this case, the reconstruction walk was repeated in the 3' direction until the 3' end of ORF2 was
309 reached. Percent identity cutoff was set at 92% for *O. palustris* and higher percent identity (97
310 to 99%) was used for *S. hispidus* to assure a satisfactory consensus for each walk and the

exclusion of older L1 elements. The 3' 300 bp of the reconstructed L1s were then used as the reference sequences for COSEG analysis described below.

B1 sequences from Rinehart *et al*. [57] were used as starting seeds for B1 analysis. The PCR-amplified B1s from *O. palustris* and *S. hispidus* were aligned with Lasergene MegAlign (DNASTAR, Madison, WI) and the consensus sequence (146 bp) was used as the reference sequence for COSEG analysis.

L1 and B1 subfamilies in *O. palustris* and *S. hispidus* were identified and characterized in similar fashion as described below and are summarized in Table S1 and S2.

The reconstructed 300 bp sequences from the 3' end of *O. palustris* and *S. hispidus* L1 ORF2 were each used as the initial L1 query sequences, and the full length B1 consensuses from each species, based on Rinehart *et al*. [57], were used as the initial B1 query sequences. *O. palustris* and *S. hispidus* MiSeq genomic DNA libraries were queried to identify homologous sequences using RepeatMasker [67] with default parameters. Hits from each search were filtered for >90% coverage of the query sequence and subsequently used for the first COSEG [67] (http://www.repeatmasker.org/COSEGDownload.html) run to identify subfamilies base on shared, co-segregating sequence variants. All COSEG runs were conducted under default parameter except as noted. Parameters were set such that at least 250 sequences were required to form an L1 subfamily and 1,000 were required to form a B1 subfamily. In order to identify older subfamilies, the consensus sequences of the subfamilies identified by the first COSEG run were used as queries to again search the *O. palustris* and *S. hispidus* MiSeq libraries using RepeatMasker. The identified sequences from the second RepeatMasker run were filtered for >90% coverage and extracted. *O. palustris* and *S. hispidus* sequences are combined and a second COSEG run was carried out on the combined sequences. To avoid the possible formation of

random subfamilies due to the short length of B1 and the high copy number of the detected sequences, the sequences required to form a subfamily was increased from 1,000 (for the former separate run) to 2,000, whereas this number for L1 remained unchanged at 250. The consensus sequences of the resulting COSEG subfamilies were trimmed to exclude ends that were not common to all subfamilies and the CpG sites were removed and, thus, treated as gaps by RepeatMasker and not counted for the divergence calculation. These modified subfamily consensus sequences were used for a final query of the individual *O. palustris* and *S. hispidus* MiSeq libraries using RepeatMasker. Sequences from this third run were assigned to subfamilies based on percent divergence and this information was stored for further analysis.

P. maniculatus genome trace files were data-mined in a similar fashion through a single round of RepeatMasker and COSEG. The *O. palustris* L1 and B1 sequences described above were used as the initial query seeds for this run. Selected *P. maniculatus* subfamilies were used to demarcate the ages of the subfamilies identified in the *O. palustris* and *S. hispidus* genomes (Figure 3).

Subfamily consensus sequences generated by the second COSEG run of the *O. palustris* and *S. hispidus* libraries were combined and aligned with MegAlign using the Clustal W method for L1 or Clustal V method for B1 and a distance matrix was calculated based on the alignment. Based on the alignment, a maximum likelihood tree was constructed using PhyML [76] with the GTR+I+G model and 100 bootstrap replicates (Figure S1). L1 and B1 sequences were then assigned to families based on the topology of the tree and a no more than 3.5% within-family pairwise distance from their subfamily consensuses for L1 and 4.4% for B1. Given that the L1 and B1 masters are constantly being replaced during evolution, perfect designation of large families is not possible. The 3.5% threshold was chosen so as to cluster closely related

subfamilies without inflating the number of families. Families are named according to their species-specificity and age: "S" indicates *Sigmodon*-specific families, "OS" for families shared by *Sigmodon* and *Oryzomys* and "OSP" for families shared by *Sigmodon*, *Oryzomys* and *Peromyscus*; numbers in family names indicates the age of a family within the family group with "1" being the youngest. Histograms of L1 and B1 age distributions were generated by R [77] histogram function using a window size of 1% (Figure 3). Percent divergence corresponding to retrotransposition peaks of individual families and subfamilies were determined by R using the kernel smoothing function with 0.4% bandwidth (Table S1 and S2).

Availability of supporting data

All data generated or analyzed during this study are included in this published article and its supplementary information files.

List of abbreviations

LINE: Long INterspersed Element

SINE: Short INterspersed Element

MYA: Million Years Ago

ORF: Open Reading Frame

O. palustris: *Oryzomys palustris*

S. hispidus: *Sigmodon hispidus*

P. maniculatus: *Peromyscus maniculatus*

Competing interests

The authors claim no competing interests.

Author's contributions

LY and HAW perceived and designed the experiment, analyzed the data and wrote the manuscript. LY prepared the DNA library for high-throughput sequencing and performed the bioinformatics analysis.

Acknowledgements

We thank LuAnn Scott for helpful discussions, editing and proofreading of the manuscript. We thank Dr. Jerzy Jurka at the Genetic Information Research Institute for offering the bioinformatics training. We thank John Brunsfeld and Dr. Celeste Brown on helpful ideas of the L1 reconstruction pipeline design. We thank Drs. Wenfeng An, Celeste Brown and James Foster for helpful comments and discussions. We thank the IBEST Genomics Resources Core for helping us to generate the high-throughput sequencing data used and the IBEST Computer Resources Core for hosting the clusters used for the bioinformatics analysis. This work was funded by National Institute of Health R01-GM38737 to HW and National Science Foundation DDIG-1210694 to HW and LY; analytical resources were provided by National Institute of Health GM103324 and GM103408. The funder had no role in study design, data collection and analysis, decision to publish, or preparation of the manuscript.

References

1. Smit AF: **The origin of interspersed repeats in the human genome**. *Curr Opin Genet Dev* 1996, **6**(6):743-748.

2. Lander ES, Linton LM, Birren B, Nusbaum C, Zody MC, Baldwin J, Devon K, Dewar K, Doyle M, FitzHugh W *et al*: **Initial sequencing and analysis of the human genome**. *Nature* 2001, **409**(6822):860-921.

3. Mouse Genome Sequencing C, Waterston RH, Lindblad-Toh K, Birney E, Rogers J, Abril JF, Agarwal P, Agarwala R, Ainscough R, Alexandersson M *et al*: **Initial sequencing and comparative analysis of the mouse genome**. *Nature* 2002, **420**(6915):520-562.

4. Furano AV: **The biological properties and evolutionary dynamics of mammalian LINE-1 retrotransposons**. *Progress in nucleic acid research and molecular biology* 2000, **64**:255-294.

5. Boissinot S, Sookdeo A: **The Evolution of LINE-1 in Vertebrates**. *Genome Biol Evol* 2016, **8**(12):3485-3507.

6. Wei W, Gilbert N, Ooi SL, Lawler JF, Ostertag EM, Kazazian HH, Boeke JD, Moran JV: **Human L1 retrotransposition: cis preference versus trans complementation**. *Molecular and cellular biology* 2001, **21**(4):1429-1439.

7. Kulpa DA, Moran JV: **Cis-preferential LINE-1 reverse transcriptase activity in ribonucleoprotein particles**. *Nat Struct Mol Biol* 2006, **13**(7):655-660.

8. Han JS, Boeke JD: **A highly active synthetic mammalian retrotransposon**. *Nature* 2004, **429**(6989):314-318.

9. An W, Dai L, Niewiadomska AM, Yetil A, O'Donnell KA, Han JS, Boeke JD: **Characterization of a synthetic human LINE-1 retrotransposon ORFeus-Hs**. *Mob DNA* 2011, **2**(1):2.

10. Han JS, Szak ST, Boeke JD: **Transcriptional disruption by the L1 retrotransposon and implications for mammalian transcriptomes**. *Nature* 2004, **429**(6989):268-274.

11. Belancio VP, Hedges DJ, Deininger P: **LINE-1 RNA splicing and influences on mammalian gene expression**. *Nucleic acids research* 2006, **34**(5):1512-1521.

12. Dewannieux M, Esnault C, Heidmann T: **LINE-mediated retrotransposition of marked Alu sequences**. *Nature genetics* 2003, **35**(1):41-48.

13. Dewannieux M, Heidmann T: **L1-mediated retrotransposition of murine B1 and B2 SINEs recapitulated in cultured cells**. *Journal of molecular biology* 2005, **349**(2):241-247.

14. Wallace N, Wagstaff BJ, Deininger PL, Roy-Engel AM: **LINE-1 ORF1 protein enhances Alu SINE retrotransposition**. *Gene* 2008, **419**(1-2):1-6.

15. Vassetzky NS, Kramerov DA: **SINEBase: a database and tool for SINE analysis**. *Nucleic acids research* 2013, **41**(Database issue):D83-89.

16. Deininger PL, Tiedge H, Kim J, Brosius J: **Evolution, expression, and possible function of a master gene for amplification of an interspersed repeated DNA family in rodents**. *Progress in nucleic acid research and molecular biology* 1996, **52**:67-88.

17. Weiner AM: **An abundant cytoplasmic 7S RNA is complementary to the dominant interspersed middle repetitive DNA sequence family in the human genome**. *Cell* 1980, **22**(1 Pt 1):209-218.

18. Ullu E, Tschudi C: **Alu sequences are processed 7SL RNA genes**. *Nature* 1984, **312**(5990):171-172.

19. Geiduschek EP, Kassavetis GA: **The RNA polymerase III transcription apparatus**. *Journal of molecular biology* 2001, **310**(1):1-26.

448 20. Schramm L, Hernandez N: **Recruitment of RNA polymerase III to its target**
449 **promoters**. *Genes & development* 2002, **16**(20):2593-2620.
450 21. Bird AP: **DNA methylation and the frequency of CpG in animal DNA**. *Nucleic acids*
451 *research* 1980, **8**(7):1499-1504.
452 22. Luo ZX, Yuan CX, Meng QJ, Ji Q: **A Jurassic eutherian mammal and divergence of**
453 **marsupials and placentals**. *Nature* 2011, **476**(7361):442-445.
454 23. Casavant NC, Hardies SC: **The dynamics of murine LINE-1 subfamily amplification**.
455 *Journal of molecular biology* 1994, **241**(3):390-397.
456 24. Pascale E, Liu C, Valle E, Usdin K, Furano AV: **The evolution of long interspersed**
457 **repeated DNA (L1, LINE 1) as revealed by the analysis of an ancient rodent L1**
458 **DNA family**. *J Mol Evol* 1993, **36**(1):9-20.
459 25. Adey NB, Schichman SA, Graham DK, Peterson SN, Edgell MH, Hutchison CA, 3rd:
460 **Rodent L1 evolution has been driven by a single dominant lineage that has**
461 **repeatedly acquired new transcriptional regulatory sequences**. *Molecular biology*
462 *and evolution* 1994, **11**(5):778-789.
463 26. Clough JE, Foster JA, Barnett M, Wichman HA: **Computer simulation of transposable**
464 **element evolution: random template and strict master models**. *J Mol Evol* 1996,
465 **42**(1):52-58.
466 27. Kramerov DA, Vassetzky NS: **Short retroposons in eukaryotic genomes**. *International*
467 *review of cytology* 2005, **247**:165-221.
468 28. Ogiwara I, Miya M, Ohshima K, Okada N: **Retropositional parasitism of SINEs on**
469 **LINEs: identification of SINEs and LINEs in elasmobranchs**. *Molecular biology and*
470 *evolution* 1999, **16**(9):1238-1250.

29. Goodier JL, Ostertag EM, Du K, Kazazian HH, Jr.: **A novel active L1 retrotransposon subfamily in the mouse**. *Genome research* 2001, **11**(10):1677-1685.

30. Hedges DJ, Deininger PL: **Inviting instability: Transposable elements, double-strand breaks, and the maintenance of genome integrity**. *Mutation research* 2007, **616**(1-2):46-59.

31. Belancio VP, Hedges DJ, Deininger P: **Mammalian non-LTR retrotransposons: for better or worse, in sickness and in health**. *Genome research* 2008, **18**(3):343-358.

32. Muotri AR, Chu VT, Marchetto MC, Deng W, Moran JV, Gage FH: **Somatic mosaicism in neuronal precursor cells mediated by L1 retrotransposition**. *Nature* 2005, **435**(7044):903-910.

33. Coufal NG, Garcia-Perez JL, Peng GE, Yeo GW, Mu Y, Lovci MT, Morell M, O'Shea KS, Moran JV, Gage FH: **L1 retrotransposition in human neural progenitor cells**. *Nature* 2009, **460**(7259):1127-1131.

34. Chow JC, Ciaudo C, Fazzari MJ, Mise N, Servant N, Glass JL, Attreed M, Avner P, Wutz A, Barillot E *et al*: **LINE-1 activity in facultative heterochromatin formation during X chromosome inactivation**. *Cell* 2010, **141**(6):956-969.

35. Cantrell MA, Carstens BC, Wichman HA: **X chromosome inactivation and Xist evolution in a rodent lacking LINE-1 activity**. *PLoS One* 2009, **4**(7):e6252.

36. Sasaki T, Nishihara H, Hirakawa M, Fujimura K, Tanaka M, Kokubo N, Kimura-Yoshida C, Matsuo I, Sumiyama K, Saitou N *et al*: **Possible involvement of SINEs in mammalian-specific brain formation**. *Proc Natl Acad Sci U S A* 2008, **105**(11):4220-4225.

37. Kunarso G, Chia NY, Jeyakani J, Hwang C, Lu X, Chan YS, Ng HH, Bourque G: **Transposable elements have rewired the core regulatory network of human embryonic stem cells**. *Nature genetics* 2010, **42**(7):631-634.

38. Morrish TA, Gilbert N, Myers JS, Vincent BJ, Stamato TD, Taccioli GE, Batzer MA, Moran JV: **DNA repair mediated by endonuclease-independent LINE-1 retrotransposition**. *Nature genetics* 2002, **31**(2):159-165.

39. Carbone L, Harris RA, Mootnick AR, Milosavljevic A, Martin DI, Rocchi M, Capozzi O, Archidiacono N, Konkel MK, Walker JA *et al*: **Centromere remodeling in Hoolock leuconedys (Hylobatidae) by a new transposable element unique to the gibbons**. *Genome Biol Evol* 2012, **4**(7):648-658.

40. Cournac A, Koszul R, Mozziconacci J: **The 3D folding of metazoan genomes correlates with the association of similar repetitive elements**. *Nucleic acids research* 2016, **44**(1):245-255.

41. Wissing S, Montano M, Garcia-Perez JL, Moran JV, Greene WC: **Endogenous APOBEC3B restricts LINE-1 retrotransposition in transformed cells and human embryonic stem cells**. *J Biol Chem* 2011, **286**(42):36427-36437.

42. Suzuki J, Yamaguchi K, Kajikawa M, Ichiyanagi K, Adachi N, Koyama H, Takeda S, Okada N: **Genetic evidence that the non-homologous end-joining repair pathway is involved in LINE retrotransposition**. *PLoS genetics* 2009, **5**(4):e1000461.

43. Gasior SL, Roy-Engel AM, Deininger PL: **ERCC1/XPF limits L1 retrotransposition**. *DNA Repair (Amst)* 2008, **7**(6):983-989.

44. Goodier JL, Cheung LE, Kazazian HH, Jr.: **MOV10 RNA helicase is a potent inhibitor of retrotransposition in cells**. *PLoS genetics* 2012, **8**(10):e1002941.

45. McLaughlin RN, Jr., Young JM, Yang L, Neme R, Wichman HA, Malik HS: **Positive selection and multiple losses of the LINE-1-derived L1TD1 gene in mammals suggest a dual role in genome defense and pluripotency**. *PLoS genetics* 2014, **10**(9):e1004531.

46. Dai L, Taylor MS, O'Donnell KA, Boeke JD: **Poly(A) binding protein C1 is essential for efficient L1 retrotransposition and affects L1 RNP formation**. *Molecular and cellular biology* 2012, **32**(21):4323-4336.

47. Taylor MS, LaCava J, Mita P, Molloy KR, Huang CR, Li D, Adney EM, Jiang H, Burns KH, Chait BT *et al*: **Affinity proteomics reveals human host factors implicated in discrete stages of LINE-1 retrotransposition**. *Cell* 2013, **155**(5):1034-1048.

48. Cordaux R, Hedges DJ, Herke SW, Batzer MA: **Estimating the retrotransposition rate of human Alu elements**. *Gene* 2006, **373**:134-137.

49. Huang CR, Schneider AM, Lu Y, Niranjan T, Shen P, Robinson MA, Steranka JP, Valle D, Civin CI, Wang T *et al*: **Mobile interspersed repeats are major structural variants in the human genome**. *Cell* 2010, **141**(7):1171-1182.

50. Yoder JA, Walsh CP, Bestor TH: **Cytosine methylation and the ecology of intragenomic parasites**. *Trends Genet* 1997, **13**(8):335-340.

51. Bourc'his D, Bestor TH: **Meiotic catastrophe and retrotransposon reactivation in male germ cells lacking Dnmt3L**. *Nature* 2004, **431**(7004):96-99.

52. Aravin AA, Sachidanandam R, Girard A, Fejes-Toth K, Hannon GJ: **Developmentally regulated piRNA clusters implicate MILI in transposon control**. *Science* 2007, **316**(5825):744-747.

538 53. Cantrell MA, Scott L, Brown CJ, Martinez AR, Wichman HA: **Loss of LINE-1 activity**
539 **in the megabats**. *Genetics* 2008, **178**(1):393-404.
540 54. Yang L, Brunsfeld J, Scott L, Wichman H: **Reviving the dead: history and reactivation**
541 **of an extinct l1**. *PLoS genetics* 2014, **10**(6):e1004395.
542 55. Casavant NC, Scott L, Cantrell MA, Wiggins LE, Baker RJ, Wichman HA: **The end of**
543 **the LINE?: lack of recent L1 activity in a group of South American rodents**.
544 *Genetics* 2000, **154**(4):1809-1817.
545 56. Grahn RA, Rinehart TA, Cantrell MA, Wichman HA: **Extinction of LINE-1 activity**
546 **coincident with a major mammalian radiation in rodents**. *Cytogenet Genome Res*
547 2005, **110**(1-4):407-415.
548 57. Rinehart TA, Grahn RA, Wichman HA: **SINE extinction preceded LINE extinction in**
549 **sigmodontine rodents: implications for retrotranspositional dynamics and**
550 **mechanisms**. *Cytogenet Genome Res* 2005, **110**(1-4):416-425.
551 58. Platt RN, 2nd, Ray DA: **A non-LTR retroelement extinction in Spermophilus**
552 **tridecemlineatus**. *Gene* 2012, **500**(1):47-53.
553 59. Boissinot S, Roos C, Furano AV: **Different rates of LINE-1 (L1) retrotransposon**
554 **amplification and evolution in New World monkeys**. *J Mol Evol* 2004, **58**(1):122-130.
555 60. Waters PD, Dobigny G, Pardini AT, Robinson TJ: **LINE-1 distribution in Afrotheria**
556 **and Xenarthra: implications for understanding the evolution of LINE-1 in**
557 **eutherian genomes**. *Chromosoma* 2004, **113**(3):137-144.
558 61. Gallus S, Hallstrom BM, Kumar V, Dodt WG, Janke A, Schumann GG, Nilsson MA:
559 **Evolutionary histories of transposable elements in the genome of the largest living**

marsupial carnivore, the Tasmanian devil. *Molecular biology and evolution* 2015, **32**(5):1268-1283.

62. Smith MF, Patton JL: **Phylogenetic relationships and the radiation of sigmodontine rodents in South America: evidence from cytochrome b**. *Journal of mammalian evolution* 1999, **6**(2):89-128.

63. Wilson DE: **Mammal Species of the World: A Taxonomic and Geographic Reference**, vol. 2: JHU Press; 2005.

64. Cantrell MA, Ederer MM, Erickson IK, Swier VJ, Baker RJ, Wichman HA: **MysTR: an endogenous retrovirus family in mammals that is undergoing recent amplifications to unprecedented copy numbers**. *Journal of virology* 2005, **79**(23):14698-14707.

65. Erickson IK, Cantrell MA, Scott L, Wichman HA: **Retrofitting the genome: L1 extinction follows endogenous retroviral expansion in a group of muroid rodents**. *Journal of virology* 2011, **85**(23):12315-12323.

66. Cordaux R, Batzer MA: **The impact of retrotransposons on human genome evolution**. *Nat Rev Genet* 2009, **10**(10):691-703.

67. Smit A, Hubley R: **RepeatMasker Open-3.0.** In.; 1996-2010.

68. Schenk JJ, Rowe KC, Steppan SJ: **Ecological opportunity and incumbency in the diversification of repeated continental colonizations by muroid rodents**. *Systematic biology* 2013, **62**(6):837-864.

69. Marshall LG, Butler RF, Drake RE, Curtis GH, Tedford RH: **Calibration of the great american interchange**. *Science* 1979, **204**(4390):272-279.

70. Smit AF, Toth G, Riggs AD, Jurka J: **Ancestral, mammalian-wide subfamilies of LINE-1 repetitive sequences**. *Journal of molecular biology* 1995, **246**(3):401-417.

583 71. Khan H, Smit A, Boissinot S: **Molecular evolution and tempo of amplification of**
584 **human LINE-1 retrotransposons since the origin of primates**. *Genome research* 2006,
585 **16**(1):78-87.
586 72. Gregory TR: **Insertion-deletion biases and the evolution of genome size**. *Gene* 2004,
587 **324**:15-34.
588 73. Magoc T, Salzberg SL: **FLASH: fast length adjustment of short reads to improve**
589 **genome assemblies**. *Bioinformatics* 2011, **27**(21):2957-2963.
590 74. **Animal Genome Size Database.** [http://www.genomesize.com/]
591 75. Cantrell MA, Grahn RA, Scott L, Wichman HA: **Isolation of markers from recently**
592 **transposed LINE-1 retrotransposons**. *Biotechniques* 2000, **29**(6):1310-1316.
593 76. Guindon S, Dufayard JF, Lefort V, Anisimova M, Hordijk W, Gascuel O: **New**
594 **algorithms and methods to estimate maximum-likelihood phylogenies: assessing the**
595 **performance of PhyML 3.0**. *Systematic biology* 2010, **59**(3):307-321.
596 77. R Core Team: **R: A Language and Environment for Statistical Computing**. In.
597 Vienna, Austria; 2013.

598

599 **Figure legends**

600

601 **Figure 1. The phylogeny of the sigmodontine rodents.** The tree is based on Schenck *et*
602 *al.* [68]. Taxa are the sampled genera in the group; tribes are indicated on the right side of the
603 taxa. Eight of the nine tribes and 12 of the 14 sampled genera by Rinehart *et al.* [57] are shown.
604 L1 and B1 activity of each taxon is demonstrated by gray scale and: black indicates active L1
605 and B1, dark gray indicates active L1 and inactive B1 and medium gray indicates the taxa where

606 L1 activity cannot be inferred and light gray indicates the taxa where L1 can be inferred to be
607 active. "o" corresponds to active L1 and B1 and "x" corresponds to inactive L1 and B1.

608 **Figure 2. The phylogenies of L1 and B1 families.** Panel A shows the L1 tree and B
609 shows the B1 tree. To reflect ages of the families, the trees were based on the distance between
610 families. The distance between any two families was calculated by taking the average pairwise
611 distance of the consensus sequences of subfamilies that belong to each family.

612 **Figure 3. The age distribution of L1 families.** L1 families in each row are arranged in
613 chronological order with the youngest families on the left. The species analyzed in each row is
614 indicated at the right. Names of families are noted on the top of each panel. L1 copy number is
615 plotted by percent divergence from the corresponding subfamily consensus in 1% windows. The
616 age of each family is approximated by the peak of the distribution. L1 copy numbers are
617 normalized as copies per three Gbp of MiSeq sequence which approximates the copy number per
618 haploid genome. Panel A shows the shared families and panel B shows the *Sigmodon*-specific
619 families.

620 **Figure 4. Comparison of L1 and B1 families spanning their extinction.** Panel A
621 presents L1 families S5, OS1 and OS2 arranged in a chronological order with the youngest
622 families on the left, and panel B presents B1 families OS1 and OSP1. The species analyzed in
623 each row is indicated at the right. Names of families are noted at the top. Copy number of L1
624 OS2 is comparable in *O. palustris* and *S. hispidus*, but more OS1 copies were detected in *O.*
625 *palustris*. Subsequently, there was a new wave of L1 retrotransposition in *S. hispidus* (family
626 S5), but no younger waves of L1 retrotransposition events were identified in *O. palustris*. B1
627 OS1 corresponds to L1 OS2 in terms of age.

628 **Figure 5. The age distribution of B1 families.** B1 families in each row are arranged in
629 chronological order with the youngest families on the left. The species analyzed in each row is
630 indicated at the right. Names of families are noted on the top of each panel. B1 copy number is
631 plotted by percent divergence from the corresponding subfamily consensus in 1% windows. The
632 age of each family is approximated by the peak of the distribution. B1 copy numbers are
633 normalized as copies per three Gbp of MiSeq sequence which approximates the copy number per
634 haploid genome.
635
636 **Supporting information**
637 **Figure S1. The maximum likelihood phylogeny of detected L1 subfamilies.**
638 Reconstructed *O. palustris* and *S. hispidus* L1s, labeled 'seed', and *P. maniculatus* subfamilies 5
639 and 6 are included as markers. The tree was reconstructed using PhyML [76] with the GTR+I+G
640 model and 100 bootstrap replicates. Bootstrap values > 80% are shown.
641 **Figure S2. The age distribution of all detected L1 and B1 sequences.** Ages of
642 sequences are approximated by their percent divergence from the corresponding subfamily
643 consensus sequences and plotted in 1% windows. Species and retrotransposon names are
644 indicated at the top of each panel.
645 **Table S1. The statistics and designation of L1 subfamilies and families.** "Ory" stands
646 for *O. palustris* and "Sig" stands for *S. hispidus*. "Peak" indicates the peak of the L1 divergence
647 distribution of the subfamily or family identified by kernel smoothing. Copy numbers are
648 normalized as copies per three Gbp of MiSeq sequence used for the search, which approximates
649 the copy number per haploid genome. Designation of families is only shown after the first
650 subfamily that belongs to it; all subsequent subfamilies belong to this family until the

651 demarcation of the next family. Characters in family names: "S" represents *S. hispidus*-specific,
652 "OS" for shared by *O. palustris* and *S. hispidus* and "OSP" for shared by *O. palustris, S. hispidus*
653 and *P. maniculatus*. Numbers in the family names reflect their ages among the family group
654 with "1" being the youngest. Copy numbers of families are rounded sums of subfamily copy
655 numbers per three Gbp of sequences and, thus, are occasionally off by one.

656 **Table S2. The statistics and designation of B1 subfamilies and families.** "Ory" stands
657 for *O. palustris* and "Sig" stands for *S. hispidus*. "Peak" indicates the peak of the B1 divergence
658 distribution of the subfamily or family identified by kernel smoothing. Copy numbers are
659 normalized by per three Gbp of MiSeq sequence used for the search. Designation of families is
660 only shown after the first subfamily that belongs to it; all subsequent subfamilies belong to this
661 family until the demarcation of the next family. Characters in family names: "OS" represents
662 families shared by *O. palustris* and *S. hispidus* and "OSP" for families shared by *O. palustris*, *S.*
663 *hispidus* and *P. maniculatus*. Numbers in the family names reflect their ages within the family
664 group with "1" being the youngest. Copy numbers of families are rounded sums of subfamily
665 copy numbers per three Gbp of sequences.
666

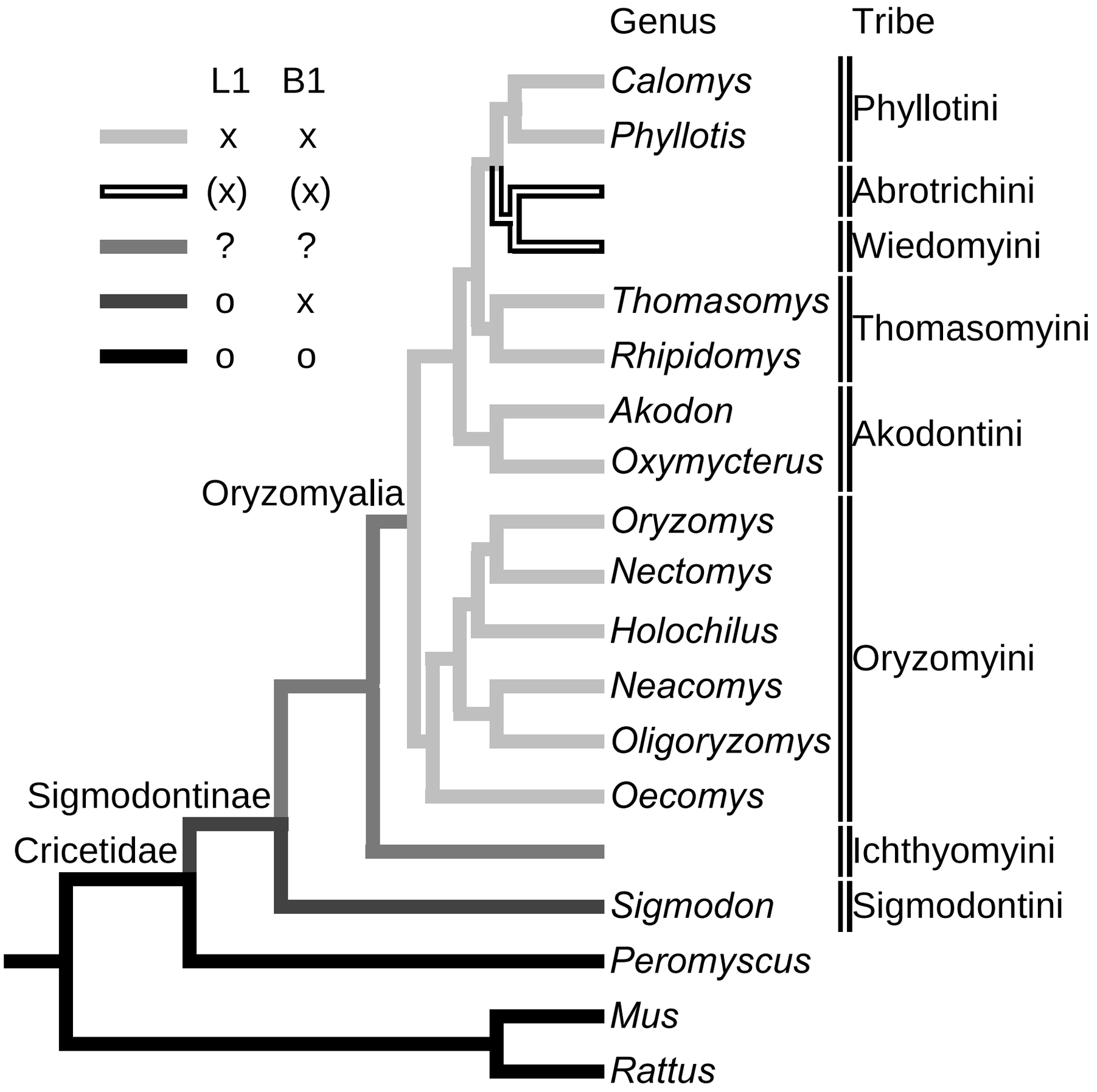
Genus
Tribe
L1
B1
x
x
(x)
(x)
?
?
o
x
o
o
Calomys
Phyllotis
Phyllotini
Abrotrichini
Wiedomyini
Thomasomys
Rhipidomys
Thomasomyini
Akodon
Oxymycterus
Akodontini
Oryzomyalia
Oryzomys
Nectomys
Holochilus
Neacomys
Oligoryzomys
Oecomys
Oryzomyini
Sigmodontinae
Cricetidae
Ichthyomyini
Sigmodon
Sigmodontini
Peromyscus
Mus
Rattus

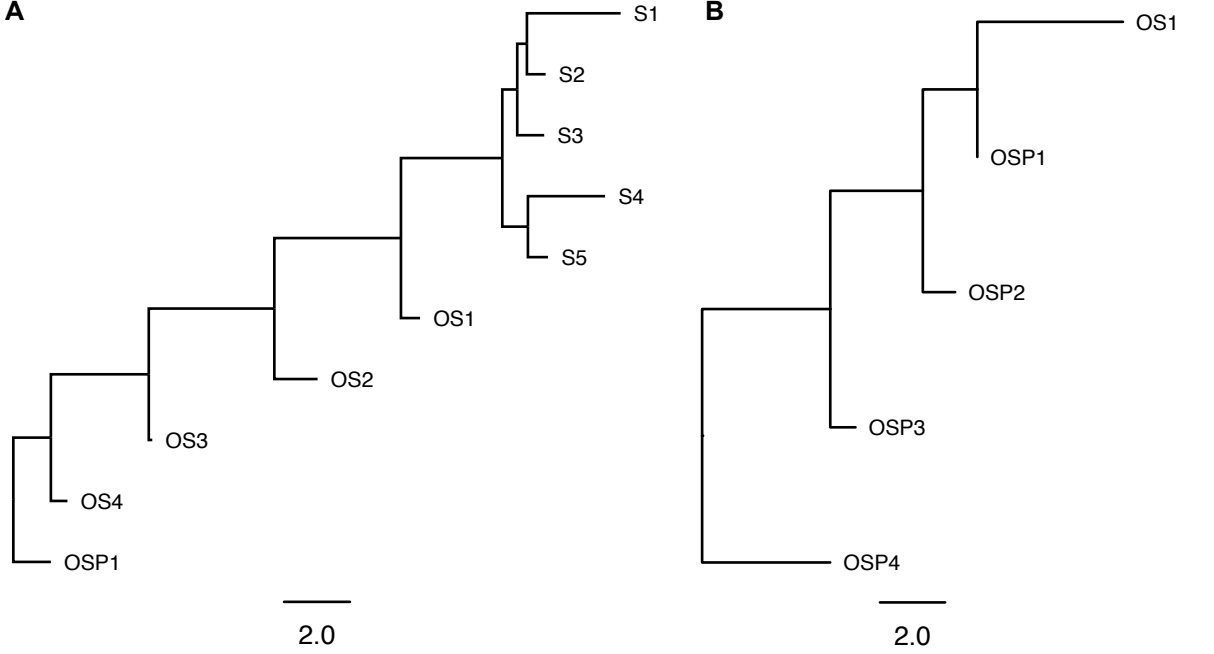
A
S1
S2
S3
S4
S5
OS1
OS2
OS3
OS4
OSP1
2.0
B
OS1
OSP1
OSP2
OSP3
OSP4
2.0

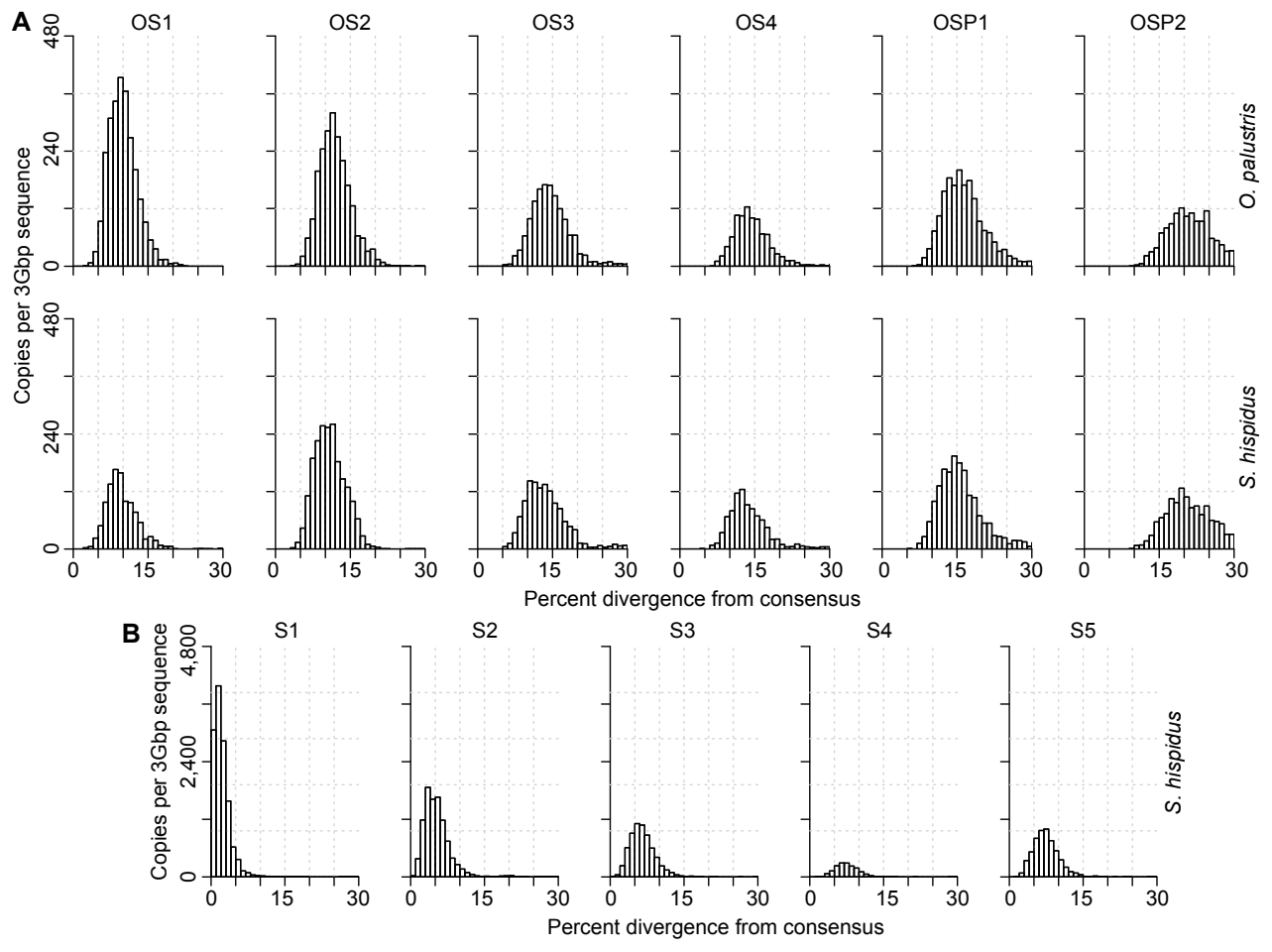
A
OS1
OS2
OS3
OS4
OSP1
OSP2
O. palustris
S. hispidus
Copies per 3Gbp sequence
0
240
480
0
15
30
Percent divergence from consensus
B
S1
S2
S3
S4
S5
S. hispidus
Copies per 3Gbp sequence
0
2,400
4,800
0
15
30
Percent divergence from consensus

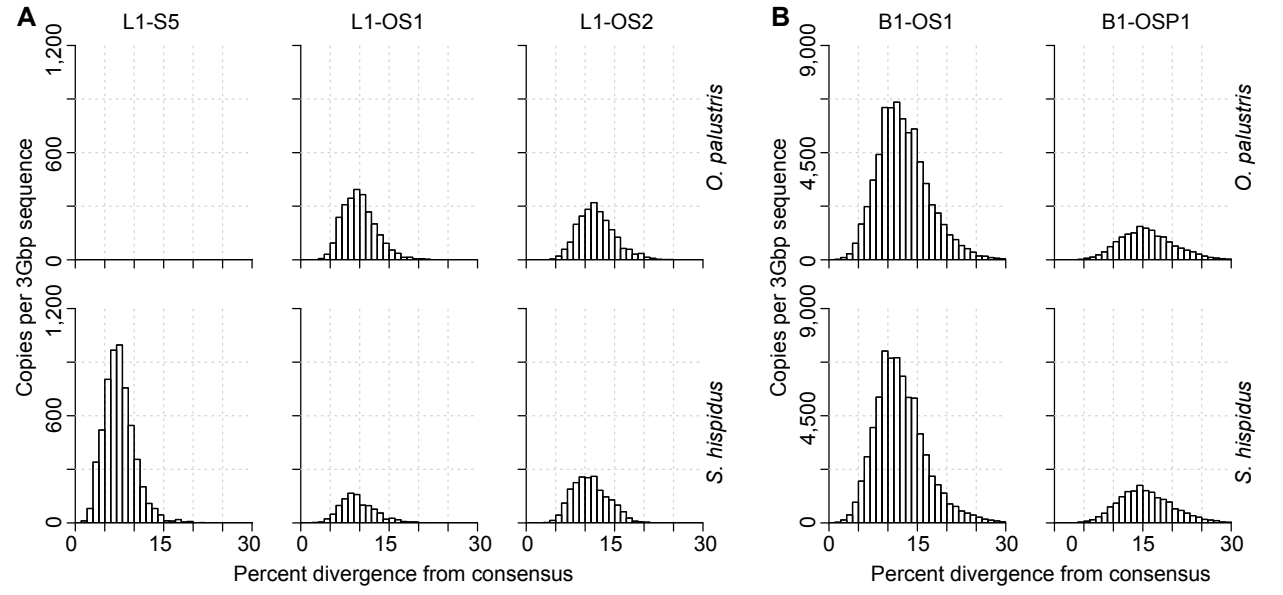
A
L1-S5
L1-OS1
L1-OS2
B
B1-OS1
B1-OSP1
O. palustris
S. hispidus
Copies per 3Gbp sequence
0
600
1,200
4,500
9,000
0
15
30
Percent divergence from consensus

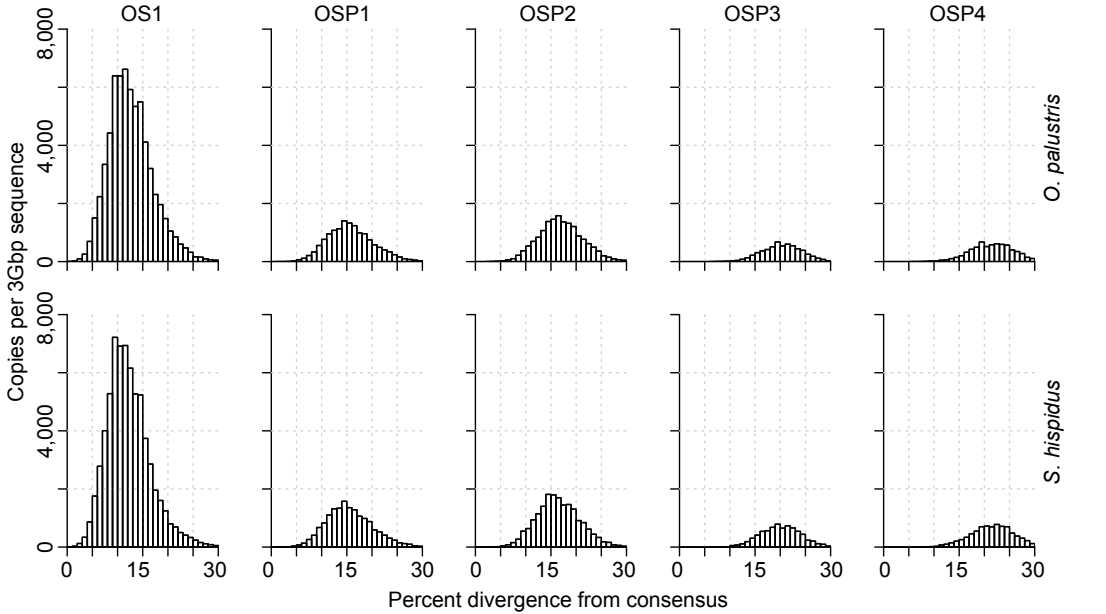
OS1
OSP1
OSP2
OSP3
OSP4
O. palustris
S. hispidus
Copies per 3Gbp sequence
0
4,000
8,000
0
15
30
Percent divergence from consensus